Experimental evaluation of the dynamic properties of a wharf structure

Rubén Luis Boroschek [a,*], Hugo Baesler [b], Carlos Vega [c]

[a] Civil Engineering Department, Universidad de Chile, Blanco Encalada 2002, Santiago, Chile
[b] PM Ingenieros S.A., Cerro Colorado 5030, Of. 703, Las Condes, Santiago, Chile
[c] GHD S.A., Apoquindo 4775, Of. 601, Las Condes, Santiago, Chile

ARTICLE INFO

ABSTRACT

This paper presents the results from a series of experimental tests carried out to determine the damping characteristics of a section of a 375 m long pile-supported wharf structure under forced excitation. The test program was designed with two primary objectives: (1) to identify the fundamental damping of the structure by using structural microvibration signals produced by tides, wind and microtremors, and (2) to evaluate the variation of the dynamic properties as a function of response amplitude by applying initial displacements of varying amplitude to the deck using a pull mechanism.

Although the wharf was designed as a series of independent deck sections, the study revealed that the non-structural frames and piping supported on top of the wharf tie adjacent sections together and have a significant influence on the dynamic behaviour, particularly in the longitudinal direction. Care must be taken in to provide sliding connections for wharf supported structures or to include the influence of these elements in the original design. From our review of the properties identified under the different excitation levels, it was determined that the wharf has relatively linear behaviour with an equivalent viscous damping of about 3%. This is a good reference damping value to be used for the analysis of the pile-supported wharf structures under operational loads and low magnitude seismic events

1. Introduction

A fundamental aspect in the seismic design process of structures is the correct estimation of their dynamic properties as a function of the expected response and level of damage. Information obtained from low level vibration testing of the existing structures can be used to improve the structural models and our understanding of their response to gravitational, operational and seismic loads.

The verification and validation of modelling recommendations for many common types of building structures has been very extensive. In contrast, much less has been done in this area regarding marine wharves. Although wharves typically have simple structural systems, their dynamic behaviour is complex due to the soil–structure interaction, the interaction between wharf segments, and the interaction between the wharf structure and the supported equipment and systems. As a result, it is difficult to define unique models for the various load states and performance levels for wharves and even more complex to correctly select the energy dissipation capabilities for the different damage states of these structures.

In the case of limited damage or operating conditions of wharves with piles, researchers have used energy dissipation values that are based on results obtained in other types of structures such as bridges and buildings, but with very limited experimental information on wharves.

For the analysis of wharves subjected to operating loads or seismic loads, where there is little or no damage, different authors and design criteria recommend the use of a reference value of about 5% of the critical damping ratio for energy dissipation [1,2]. Benzoni and Priestley [1] used a critical damping ratio between 5% and 7.5% for moderate or medium response levels, which is increased to 10%–20% in cases of extreme demand and high damage levels. Donahue et al. [3] has used a similar value of 10% in cases of extreme demand and energy dissipation levels. However, some authors consider damping values of about 5% for damage situations (e.g. [4]) when nonlinear elements are added in the analytical model with intrinsic energy dissipation. In general, it is accepted that for modelling purposes, values higher than 5% should be used when there is extensive damage [5]. The International Navigation Association recommends equivalent damping values derived from hysteretic damage models and, up to a certain level, discarding the base viscous contribution [6]. Taking this into account, equivalent values between 10% and 20% of critical damping ratios are considered.
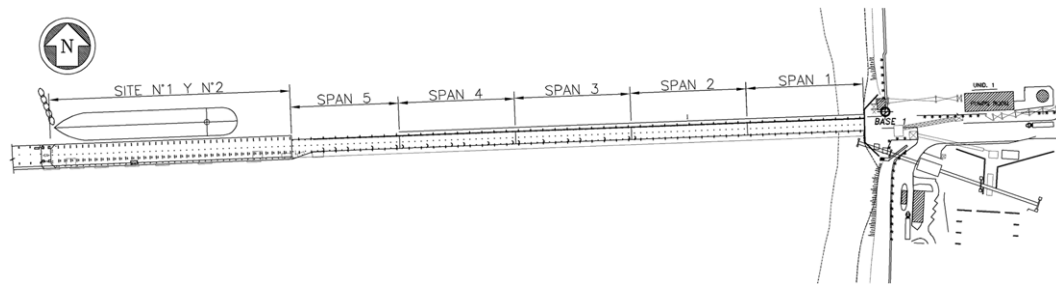
Although the values mentioned above are commonly accepted by professionals, they must be experimentally validated. Due to

* Corresponding author. Tel.: +56 29784372; fax: +56 26892833.
E-mail addresses: rborosch@ing.uchile.cl (R.L. Boroschek), hbaesler@pmingenieros.cl (H. Baesler), cvega@ghd.com (C. Vega).

(a) Aerial view looking south.

(b) General view.

Fig. 1. Ventanas port.

their large size and complexity, this validation must be made directly in the existing wharves instrumented with strong motion sensors. Unfortunately, the number of instrumented wharves is relatively small and only a few of these have been subjected to moderate or severe earthquakes. This has led to the development of controlled full-scale testing, where a wharf is temporarily instrumented and the response to different demands are measured and analyzed.

These tests can be done using ambient excitations, such as tides, wind and the operational loads, or external force excitations, such as imposed displacements, impacts, forced harmonic excitations, etc. One of the limitations of the experimental tests is that demands generated by small magnitude external excitations are considerably lower than demands expected in a severe seismic event. Despite this, the information gained from these tests allows for better calibration of important variables used in analytical models.

In this work, we present results from a series of ambient and forced vibration tests to identify the damping properties on an existing pile-supported wharf structure at Ventanas Port in the Bay of Quinteros, Chile. The study also provides a comparison of different experimental techniques and their relative advantages and disadvantages for assessing the dynamic properties of wharf structures.

2. Wharf description

The Ventanas Port wharf is located in the Bay of Quinteros, 130 km from Santiago, in central Chile. The wharf includes an access bridge and berths. The access bridge is 375 m long by 8.3 m wide and was built in the mid-1960s. It has 5 independent sections: 4 measuring 76 m in length and one measuring 71 m in length, with similar pile arrangements that run deeper as the wharf stretches out into the ocean (Fig. 1). An expansion joint of 125 mm separates the sections. The structure of each section is made up of a 30 cm thick reinforced concrete slab supported on 3 longitudinal steel beams embedded in concrete that are supported on piers located every 4 m.

Two types of bents that alternate along the length of the wharf were used for each section (Fig. 2(a) and (b)). Type 'A' bents are formed by 5 tubular-shaped steel piles — three vertical piles (457 mm diameter) and two inclined or battered piles (305 mm diameter). These piles are connected at deck level with a steel transverse beam (W36 × 135) embedded in concrete with a total cross section of 90 × 186 cm. Type 'B' bents are similar to Type 'A' bents, but without the two inclined piles. The sections closest to the beach have vertical piles gradually decreasing in diameter to 406 mm. These piles are connected at deck level by a steel transverse beam (W24 × 68) embedded in concrete with a total cross section of 90 × 96 cm.

The wharf supports various relatively tall steel structures that make up the support systems for three conveyor belts, two cooling ducts, and three fluid transport pipes (Fig. 3). The three conveyor belts carry solid bulk material (coal, grains, copper concentrate and clinker). The first, second and third pipes transport fuels and by-products, liquid bulk material, and sulphuric acid, respectively. These systems weight approximately 3400 kN. The ducts transports sea water, with an approximate weight of 4000 kN, for cooling purposes of a nearby thermoelectrical plant. From an inspection of each wharf segment, the estimated weight of the top of the deck systems and components is approximately 8400 kN; this represents 39% of the total weight of the test section of the wharf.

3. Experimental test description

The objective of the study was to determine the fundamental modal properties, especially period and critical damping ratio. Two experimental techniques were used: Pull-Back (or initial conditions) Testing and low amplitude Ambient Vibrations Testing.

The Ambient Vibrations Test is based on the measurement of the response of a structure under natural excitations (wind, tides,
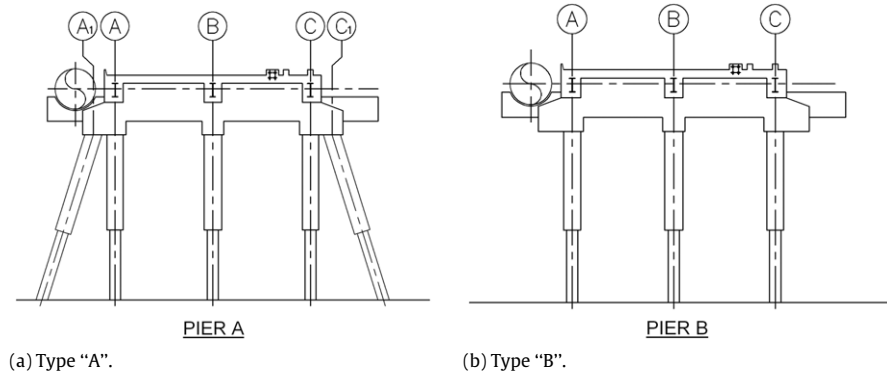
(a) Type "A".   (b) Type "B".

Fig. 2. Typical pier arrangement.

Fig. 3. General view of top deck systems. Note the pipes and frames running in the longitudinal direction that may provide some degree of restraint between adjacent sections.

usage, etc.). It is relatively fast and economic, but not always accepted by professional designers because the identification is made with relatively low amplitude vibrations (maximum acceleration amplitudes of about 0.005 g). These amplitudes are not representative for structures that have nonlinearities such as the interaction with non-structural elements or neighbour structures or nonlinearities of materials that are only present at larger amplitudes. A procedure to generate higher amplitudes is through Pull-Back testing (imposition of initial conditions). A description of these tests and their signal analysis procedures are described below.

3.1. Pull-Back test

Pull-Back testing consists of pulling on the structure to impose initial conditions (displacement and velocity) to a structure in order to generate an important response of the system. From the analysis of the response decay it is possible to determine the dynamic properties of the structure. This type of test presents several difficulties when applied to large existing structures in operation [7,8]. The principal difficulty is related to the application of the load, which requires a strong support point and an accurate determination of the load magnitude to prevent damage to the test structure. Additionally, due to safety reasons, the test execution typically requires stopping the operations along the structure. This situation necessarily implies the development of detailed studies about the condition of the structure and preparation of predictive computer models. All this requires longer preparation and execution times for the test and therefore, higher costs and risks.

3.1.1. Parameter identification

To identify the modal parameters from the structural response to initial conditions, it is normally assumed that the decay corresponds to a viscoelastic mechanism and therefore the response is the sum of harmonic functions (as in the case of several excited degrees of freedom) with different frequencies, but whose amplitude decreases exponentially. The most common identification techniques are the logarithmic decrement techniques used in single-degree-of-freedom (SDOF) systems and the Ibrahim Time Domain Method (ITD) for multi-degree-of-freedom (MDOF) systems [9].

The SDOF method can be used for SDOF systems, MDOF systems where only one mode is excited, or MDOF systems where it is possible to generate signals associated with a single mode through filtering of the response record. Damping can be obtained based on the amplitude variation between successive or non-successive maxima or, in a more robust manner, from the slope of a curve corresponding to the maximum amplitude values (v_n) as a function of the sequential numbers of those maxima (n) (i.e. a plot with a vertical logarithmic axis and a linear horizontal axis, $\ln(v_n)$vs · n). For the perfectly viscous case, the curve generated corresponds to a straight line. The slope of this curve is the value of the damping divided by the value of π. In practical cases, and in the presence of instrumental noise and influence of various energy dissipation mechanisms, it is recommended to create a best-fit straight line to determine the slope. Also a segmental analysis can be used to establish the effects of amplitude on energy dissipation as a function of amplitude. Then from the shape of the decay response, it is possible to know if the system presents a classical energy dissipation mechanism, such as friction or viscous behaviour, and whether the response parameters change with the amplitude of the motion.

When it is not possible to use the SDOF model, it is necessary to identify all the frequencies, damping values and participation factors simultaneously. In ITD, an adjustment to the observed decay response is made through least squares; see the detailed procedure in Ibrahim Time Domain Method (ITD) for multi-degree-of-freedom systems [9].

3.1.2. Design of the pull test

A special system was designed to carry out the Pull-Back Test [10]. This system was located between two sections of the wharf (Fig. 4(a)). The system consists of two bolted base plates, (Fig. 4(b)), located close to the wharf section expansion joint. During the test, these two plates are pulled towards each other using a connecting element and a hydraulic jack. In the middle of the connector there is a steel plate designed to break and act as a fuse (Figs. 5–7). The hydraulic jack pulls the connecting element
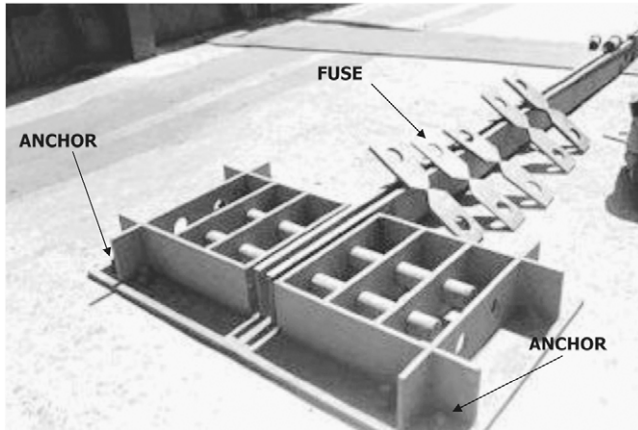
(a) Installation.
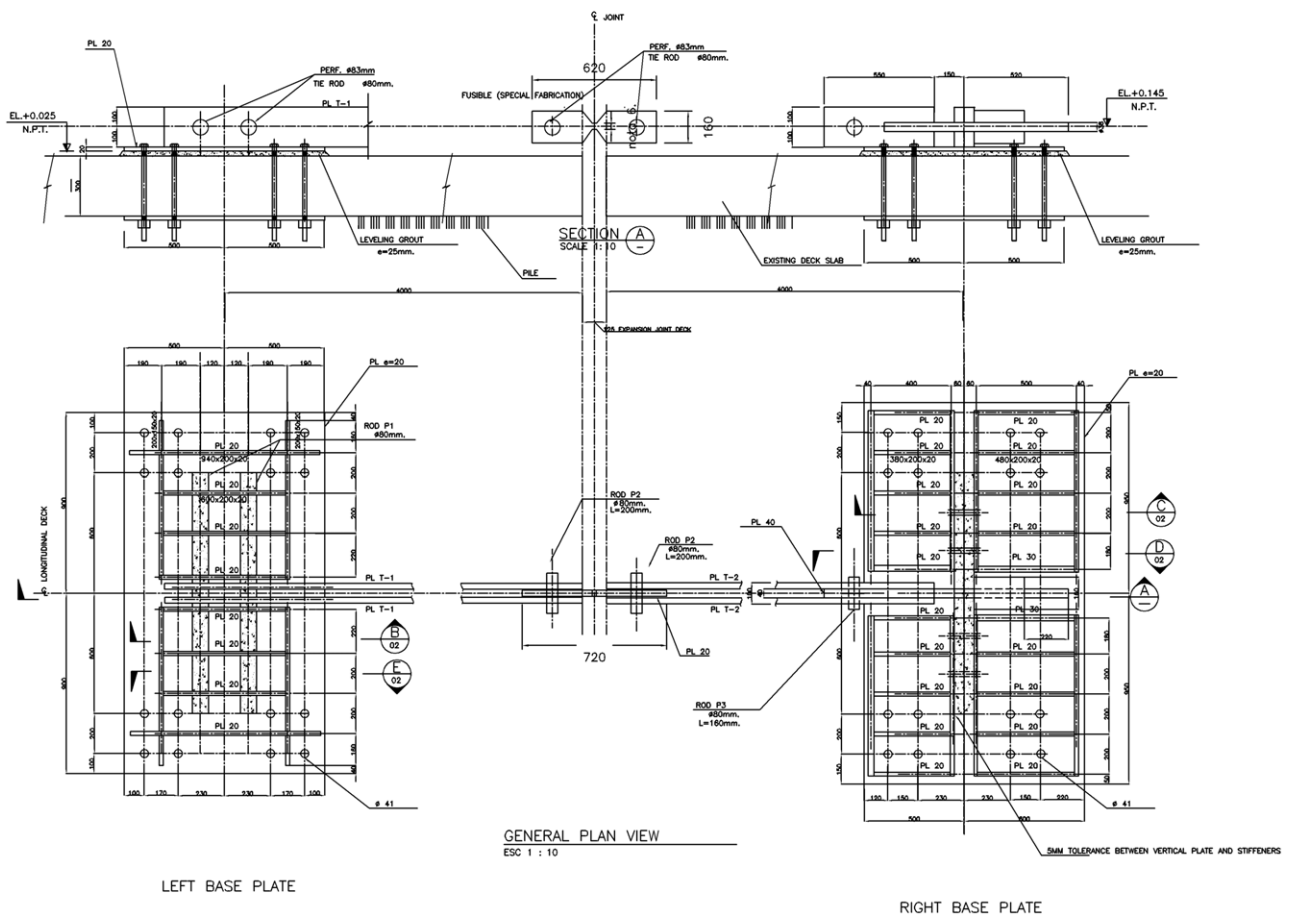
(b) Structural details [10].
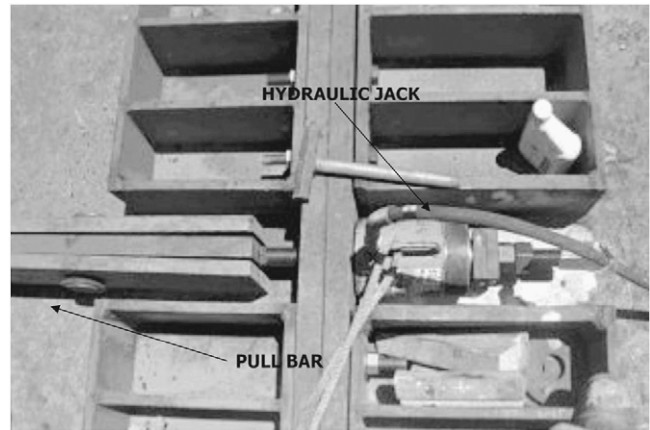
Fig. 4. Pull system.

until the fuse fails. The imposed displacement and sudden release produce a vibration on the structure.

The maximum fuse capacity was selected, so no damage was induced in the wharf system. This value was determined from a simplified analytical model of the different sections of the wharf structure. For this model only the deck slab, beams and piles were included for stiffness calculations. Slab stiffness was based on its 30 cm thickness, an overall plan dimension. Piles were considered with the 9 mm wall section reduced by 2 mm to account for corrosion effects. In order to consider soil effects, different equivalent full fixity lengths were considered
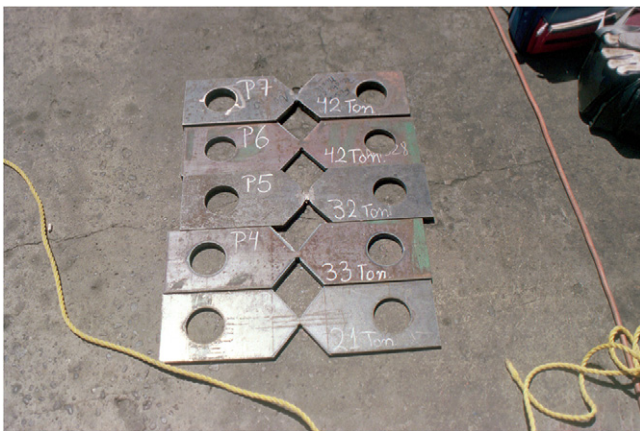
for the piles. Equipment and top structures were considered only as mass. The envelope of higher pull force and displacement was used to design the pull system and to control damage due to the relative displacements at the expansion joint [10]. The controlling variable was the capacity of the deck at the location of attachment of the pull plates. As a result of the parametric study the pulling system was designed for a static force of 500 kN and a maximum fuse capacity of 420 kN. To account for the impact force, an amplification factor of two times the static load was used in the design, resulting in a total design force of 1000 kN.

(a) General view.

(b) Hydraulic Jack installation details.

Fig. 5. Pull system.
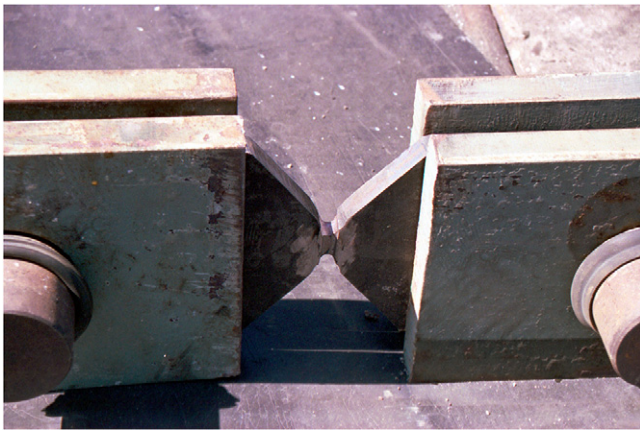
Fig. 6. Fuse setup details.
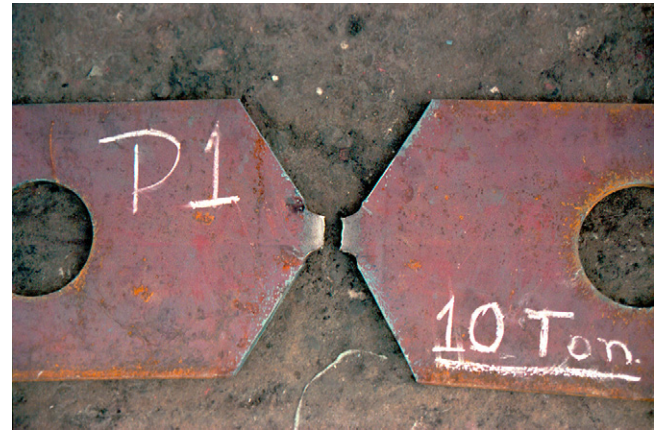
Fig. 8. Fragile fuse rupture. Due to material low ductility practically no section reduction exists before failure.

Table 1
Technical specification for the fuse material.

Brand	Thyssen
Material	Steel alloy
Name	XAR prime
Composition	20MnCr6-5
Creep tensile strength	0.7 MPa
Deformation	13%
Rupture strength	1 MPa

3.2. Ambient microvibrations

The structures are permanently excited by different sources of natural origin (wind, tides, etc.). Through the analysis of these vibrations, it is possible to determine the dynamic properties of the structure. To record motions under ambient conditions, it is necessary to position a sensor that is sensitive enough to detect small structural vibrations. Because no additional loads are applied to the system, it is possible to develop the experimental part of the study very quickly and at a very low cost. In general, the functionality of the structure to be monitored is not altered and there is no risk to the structure itself or to bystanders. Due to this, it is a very appealing technique when the structure shows an essentially linear behaviour or when it is useful to evaluate the structural response under actual operating conditions.

There are several system identification techniques that use ambient vibration records [11]. The identification procedure can be classified as parametric or non-parametric if an analytical

Fig. 7. Fuse details.

3.1.3. Fuse design

The fuses were designed with a fragile material (Table 1) to guarantee the maximum force, the failure section and the sudden release (Fig. 8). Fuses of different thicknesses, widths and anchoring types were tested until reaching an acceptable rupture mechanism that can be considered safe for the wharf system. To guarantee the maximum force, three (3) fuses were prepared from each steel plate, one of which was tested in a universal test machine to validate their rupture value.

(parametric) model of the dynamic characteristics is used. Essentially, for the non-parametric technique, the time and frequency properties of the records are identified and are later associated with the structure's modal parameters using an expert opinion.

3.2.1. Non-parametric frequency (NPF) method

In the frequency domain, the non-parametric identification of the dynamic properties is made by obtaining the Fourier Transform, the power spectral density, the coherence and the amplitude and phase of the response signals. To estimate reliable results, statistical averages with appropriate time windows are required. Details of this method can be found in Refs. [11–14].

To identify the dynamic properties of the structure using NPF, it is necessary to identify the predominant frequencies and the amplitude and phase relationship among signals for the given frequencies. This information will indicate the predominant frequencies and associated operational mode shapes.

The equivalent viscous damping (β) can be obtained using the bandwidth method, [14] where

$$\beta = 0.5\Gamma(1 - 0.375\Gamma^2) \tag{1}$$

and

$$\Gamma = \frac{f_2^2 - f_1^2}{f_2^2 + f_1^2} \tag{2}$$

f_1 and f_2 are the frequencies that correspond to half the maximum value of the Power Spectral Density of the predominant frequency being analyzed.

Extreme care must be exercised when applying this simple procedure because the results are highly dependent on the filter used to process the response signal, sampling frequency, time window and duration of the record. For this method to have relatively reliable values of damping, it is necessary to have long-term stationary records from which to obtain a large number of averages with long time windows. Diehl [12] suggests a minimum of 32 time window averages. He also presents a formula to estimate the minimum record length based on the value of damping and natural frequency of the structure. In our practice, a minimum of 10 min is used and the preferred record duration is one hour. Additionally if it is assumed that the structure is excited by a white noise source it is possible to correct the distortion of the identified damping value due to window shape, duration and number of averages as shown in [14].

3.2.2. Stochastic Subspace Identification (SSI)

Stochastic Subspace Identification (SSI) is a time domain parametric technique [19,15]. The method is based on the study of a system with two-equations where the first one is associated with the dynamic equilibrium (Eq. (3)), and the second one is associated with the data obtained, for a given sensor array, in the actual structure or observed data, Eq. (4).

$$M\ddot{q}(t) + C\dot{q}(t) + Kq(t) = f(t) \tag{3}$$

where $q(t)$, $\dot{q}(t)$, $\ddot{q}(t)$ represent the displacement, velocity and acceleration vectors, respectively.

M, C, K are the mass, damping and stiffness matrices of the model and $f(t)$ is the excitation.

$$y(t) = H_a\ddot{q}(t) + H_v\dot{q}(t) + H_d q(t) \tag{4}$$

where the observed response data is $y(t)$ and H_a, H_v, H_d are the location matrices for the output data for acceleration, velocity and displacement, respectively. They are matrices composed only of zeros and ones.

We can rewrite Eq. (4) as a first order equation.

$$\dot{x}(t) = A_c x(t) + f_c(t) \tag{5}$$

where

$$A_c = \begin{pmatrix} 0 & I \\ -M^{-1}K & -M^{-1}C \end{pmatrix}, \qquad f_c(t) = \begin{pmatrix} 0 \\ M^{-1}f(t) \end{pmatrix},$$

$$x(t) = \begin{pmatrix} q(t) \\ \dot{q}(t) \end{pmatrix}. \tag{6}$$

Eq. (5) represents the state equation in the state-space system, and subscript c represents continuous time.

For our case, the ambient excitation is unknown. For the case in which we only know the system's output signal, the state-space system of the equation – in its digital data (non-continuous) adapted version – is as follows [15]:

$$\begin{aligned} x_{k+1} &= Ax_k + w_k \\ y_k &= Hx_k + v_k \end{aligned} \tag{7}$$

where w_k is the "noise" process due to the model's disturbances and uncertainties, and v_k is the noise measurement associated with the sensor's uncertainty at time step k. x_k, y_k are $x(t), y(t)$ at time $t = k\Delta t$, and

$$A = e^{A_c\Delta t}$$
$$H = [H_d - H_a M^{-1}K \; H_v - H_a M^{-1}C].$$

The input signal is implicit in the noise terms.

From the observed data, it is possible to build matrices that allow matrix A to be obtained through an appropriate decomposition. In our case, we have used the N4SID routine [16] included in the Matlab software System Identification Toolbox.

A basic identification problem with this procedure is to estimate the number of modal parameters that actually participate in the response and how to differentiate them from the ones generated by the signal's noise. For this purpose, decomposition and analysis of the matrix's singular values is needed. They are built in a sequential manner, considering for each case an increasing number of degrees of freedom. The modal properties recognized (period, damping and modal form) in each identification are compared to the former case; they are considered to have reached a stable value if they do not vary more than a certain percentage. For example, in our case we have used

$$\frac{|f(ngdl) - f(ngdl + 1)|}{f(ngdl)} < 0.01$$
$$\frac{|\beta(ngdl) - \beta(ngdl + 1)|}{\beta(ngdl)} < 0.05$$
$$\frac{|MAC(ngdl) - MAC(ngdl + 1)|}{MAC(ngdl)} < 0.02 \tag{8}$$

where

f, β, MAC is the frequency, critical damping ratio and the Modal Assurance Criteria of the mode under study [17,18].

$ngdl$ is the number of degrees of freedom considered in matrix A.

4. Description and result of the measurements

From the preliminary analytical model it was concluded that the controlling predominant motions where the first longitudinal and first transverse modes. To measure these motions with microvibrations, four inertial velocity sensors were located on the deck, three of them in the transverse direction and one in the longitudinal direction (Fig. 9(a)). The sensor used for the ambient vibration monitoring attenuates amplitudes below 1 Hz. In practical terms, this limits the observation of motion below 0.5 Hz.
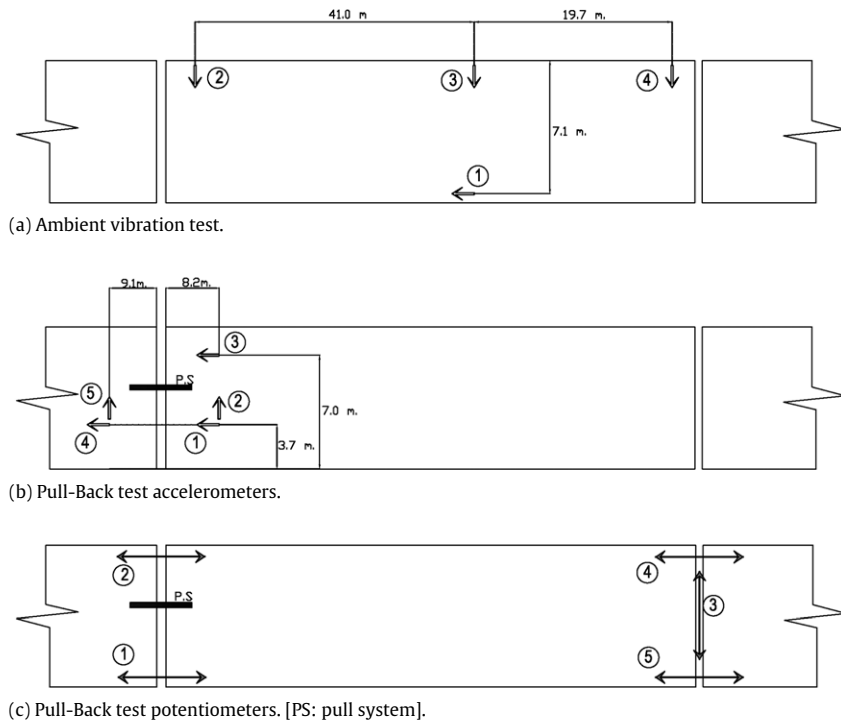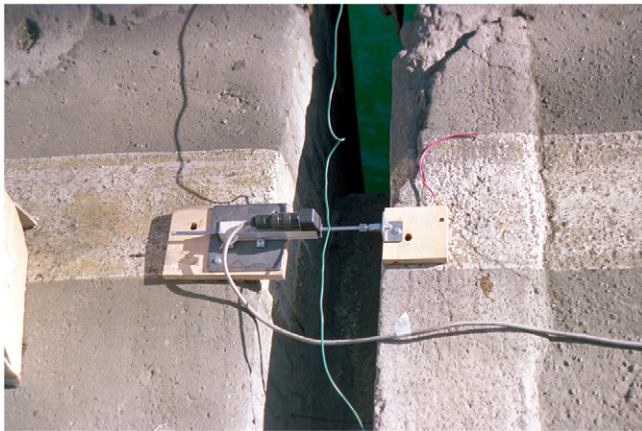
(a) Ambient vibration test.

(b) Pull-Back test accelerometers.

(c) Pull-Back test potentiometers. [PS: pull system].

Fig. 9. Sensor distribution and orientation.

Fig. 10. Displacement sensor installation between structural joints.

Fig. 11. Ambient vibration records of deck.

For the Pull-Back Test inertial accelerometers and relative displacement instrumentation was used (Fig. 9(b) and (c)). The displacement sensors were located in the expansion joints (Fig. 10). Accelerometers were distributed along the deck in the longitudinal and transverse directions. All the instrumentation was installed to measure horizontal motions. Vertical motions were not considered important due to the rigid structural beams used at deck level.

4.1. Ambient vibration test

4.1.1. Non-parametric frequency study results

For the non-parametric analysis, ambient microvibrations were used (Fig. 11). To generate the Power Spectrum Density a 60 s Hanning window was used (Fig. 12). Fig. 13 presents the frequency and damping estimation as a function of the number of windows. It is interesting to observe that the damping and frequency values are nearly constant after 30 window averages. This value is in
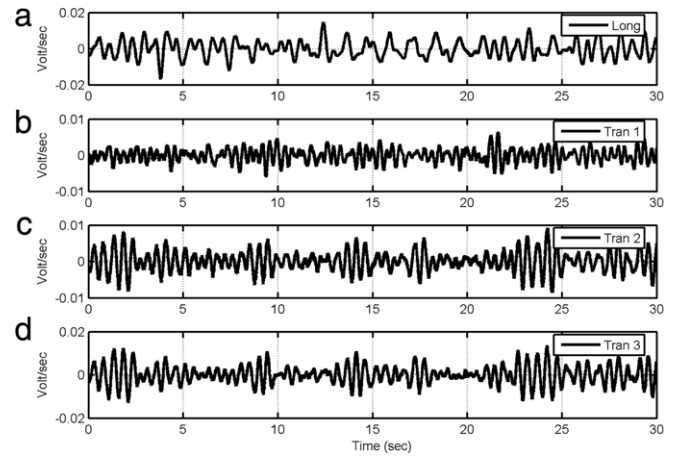
agreement with the recommendation made by Diehl [12] that the minimum number of windows is about 32.

The frequency and damping results are presented in Table 2. In Fig. 12, four predominant frequency bands are observed: 0.8–0.85 Hz; 1.66 Hz; 2.33 Hz; and 2.77–2.81 Hz. With this test and the limited distribution of sensors used it is not easy to identify the structural characteristics associated with these predominant frequencies (later, with the results from the Pull-Back tests, we confirm some interpretations made from these results), but it is possible, however, to establish the following conclusions:

- The longitudinal motion component presents amplitudes that are considerably larger than the transverse amplitudes. This is reasonable because the transverse direction motions are limited by the battered piles. Nevertheless some transverse deck flexibility and torsion is observed from the different amplitudes and frequencies in the transverse motions (Fig. 12). Also there is coupling between wharf segments due to the presence of the top deck structures and pipes and because
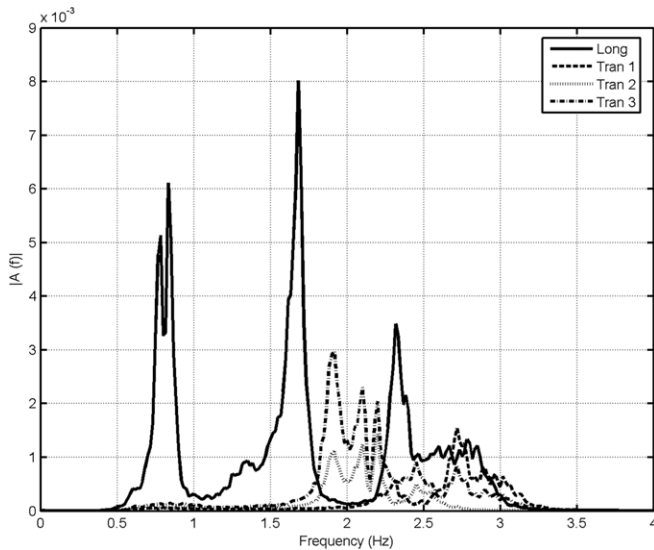
Fig. 12. Power spectral density of the top of deck ambient vibration records.

of a longitudinal connecting beam that crosses the wharf joints.

- The frequency with the highest amplitude corresponds to the 1.66 Hz predominantly longitudinal component. This frequency is associated with an in-phase movement between deck sections.
- Using the bandwidth method, we can estimate a 3% critical damping ratio for the 1.66 Hz longitudinal first predominant motion (Fig. 14).
- An additional longitudinal predominant motion, 2.33 Hz signal, shows similar damping. However due to modal interference effects and the method used, that does not uncouple the contribution of the different modes, this is not considered to be a reliable value.
- Motion with frequencies between 2.77 and 2.81 Hz correspond to anti-symmetrical vibration between the different deck sections. This motion has transverse and longitudinal coupled effects.
- Other predominant frequencies below 1 Hz in the longitudinal direction can be associated with the structures mounted on top of the wharf deck and some attenuated ocean wave motion.

4.1.2. Stochastic subspace identification SSI results

For the SSI method six consecutive segments of 10 min of the data were used. Final estimates for frequency and damping were obtained from the average of the values determined for each time segment. In Table 2 the average and the minimum and maximum values are presented. The results also are shown in the stability diagram that considers the three estimated variables (frequency, damping and MAC), Figs. 15–17. In this diagram, there is a graphical representation only for the frequencies that at least fulfil one of the stability conditions.

These figures also have a histogram that includes all the stable frequencies, which are estimated by the model despite the fact that they do not necessarily fulfil the three stability conditions. In addition, the Power Spectrum curve associated with one of the signals is shown to help identify the frequencies with the highest energy in the system.

In Fig. 15, where only the longitudinal sensor is considered, there are several frequencies (with average values 0.83, 1.68, 2.31 and 2.82 Hz). The highest amplitude signal (1.68 Hz) that can be associated with a possible longitudinal predominant mode. There
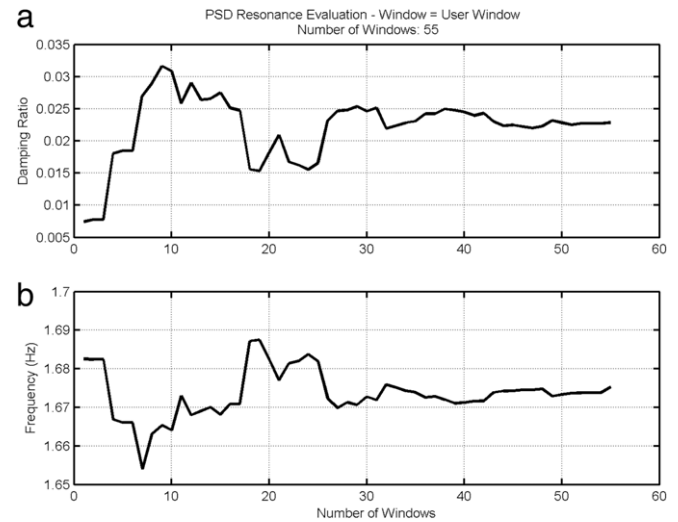

Fig. 13. Identified frequency and damping as a function of number of time windows included in spectral average.
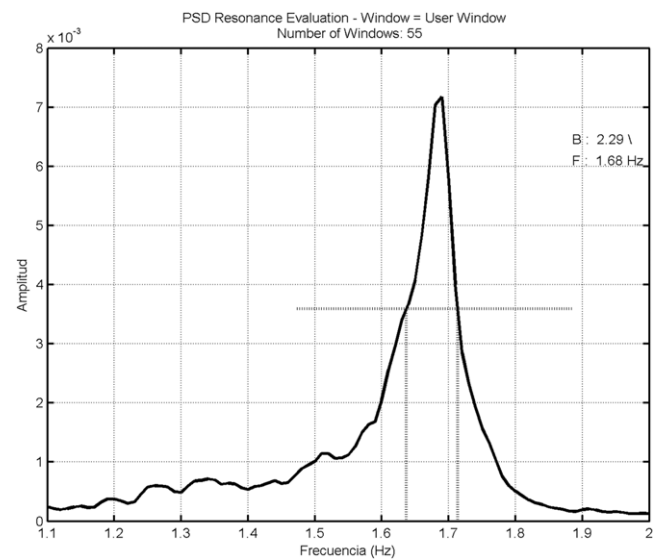

Fig. 14. Damping estimation from ambient record. Power Spectral of longitudinal record. Bandwidth and corner frequencies are indicated in plot.

are several predominant frequency for the transverse–torsional directions (1.9, 2.11, 2.20, 2.49 and 2.7 Hz), Fig. 16.

In Fig. 17, where longitudinal and transverse sensors are included, we noticed that there are several frequencies between 1.9 and 2.5 Hz with damping that oscillates between 2.8% and 5%. In addition, there are frequencies close to 2.7 and 2.8 Hz that show very different damping values.

4.2. Pull-Back test results

Seven Pull-Back tests were carried out with difference maximum apply forces, varying between 100 and 420 kN. Fig. 18 presents the longitudinal acceleration before and during the Pull-Back Test with a maximum load of 420 kN. In this figure it is possible to observe, before the relative large acceleration produced by the sudden release of the load, that the movement of the wharf is affected by sea waves, which showed a period of nearly 11–18 s and amplitudes of 0.0005 g (Fig. 19). The accelerations reached during the Pull-Back test on the measurement points are not higher than 3% g in a frequency band lower than 50 Hz.

Table 2
Comparison of frequency and damping determination using different methods.

Shape	NPF		Pull-Back		SSI	
	Freq (Hz)	Damping β	Freq (Hz)	Damping β	Freq (Hz) Average (Extreme values)	Damping β Average (Extreme values)
1	0.8–0.85	ND	–	–	0.84 (0.80–0.85)	ND
2	1.66	0.03	1.63 (1.60–1.66)	0.03 (0.02–0.03)	1.68 (1.64–1.70)	0.03 (0.02–0.04)
3	–	–	–	–	1.90 (1.87–1.92)	0.03 (0.02–0.03)
4	–	–	–	–	2.11 (2.11–2.12)	0.02 (0.01–0.03)
5	2.33	ND	–	–	2.31 (2.29–2.32)	0.03 (0.02–0.03)
6	–	–	–	–	2.49 (2.44–2.53)	0.03 (0.01–0.03)
7	2.77–2.81	ND	2.74 (2.63–2.86)	0.04 (0.04–0.05)	2.82 (2.78–2.84)	0.05 (0.03–0.06)

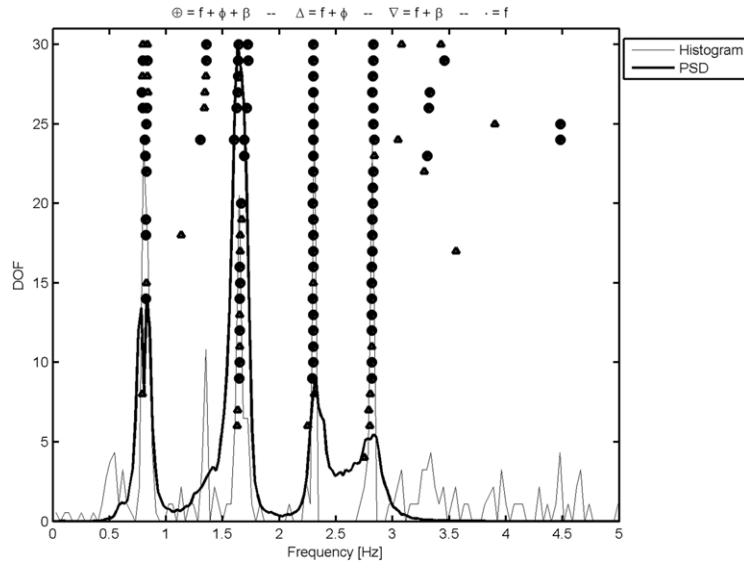ND Damping values for this frequency show large variations or the methods is not applicable.

Fig. 15. Stability diagram. Longitudinal sensor only. When frequency (f), MAC (ϕ) and damping (β) does not change between consecutive DOF, according to stability criteria, a crossed circle ($\oplus$) is indicated. Other symbols used to indicate partial stability ($\triangle$, ∇, $\bullet$) are indicated on top of the figure.
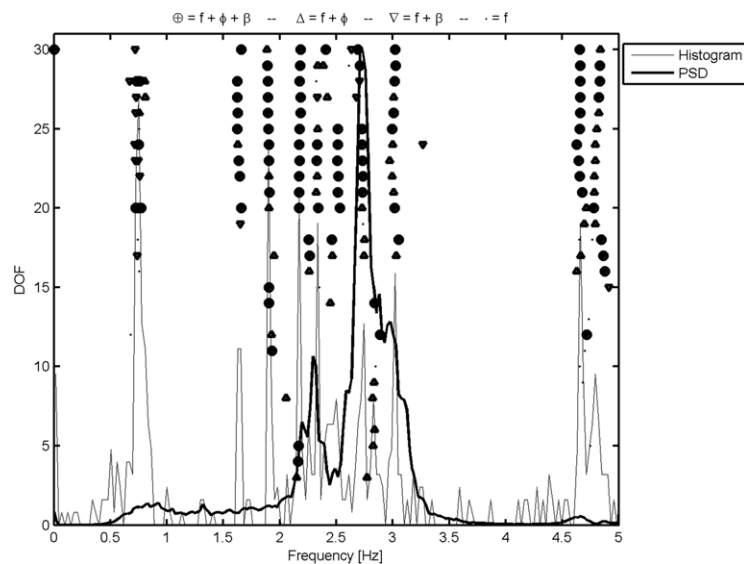

Fig. 16. Stability diagram. Transverse sensors only.

Fig. 20 presents the acceleration response to the various loads. In global terms, the difference in the acceleration response for the various initial forces is not very significant.

It can be observed that the acceleration signals do not show much noise and that they are formed by more than one decaying harmonic frequency. A time–frequency decomposition of the decay clearly indicates the presence of two predominant signals with a relatively constant frequency in the face of various levels of acceleration amplitude (Figs. 21 and 22). This means that the system had a linear response.

To determine the system's damping, the logarithmic decrement was used. In this case, to use the logarithmic decrement method,
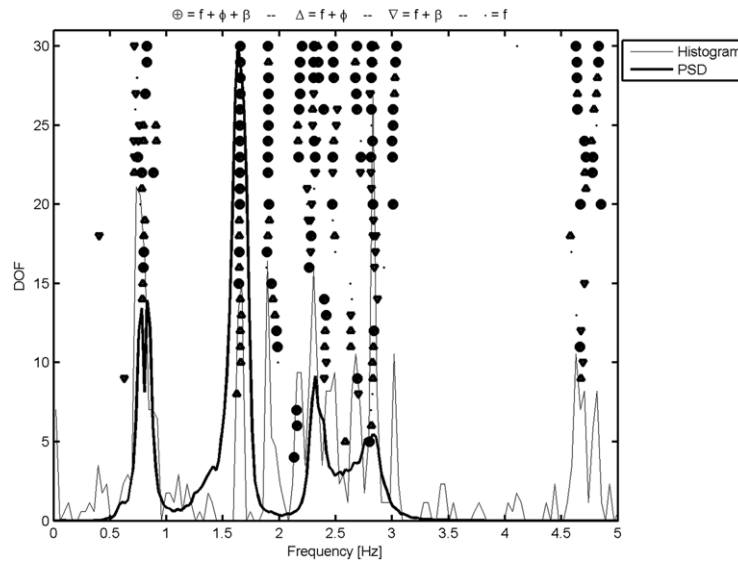
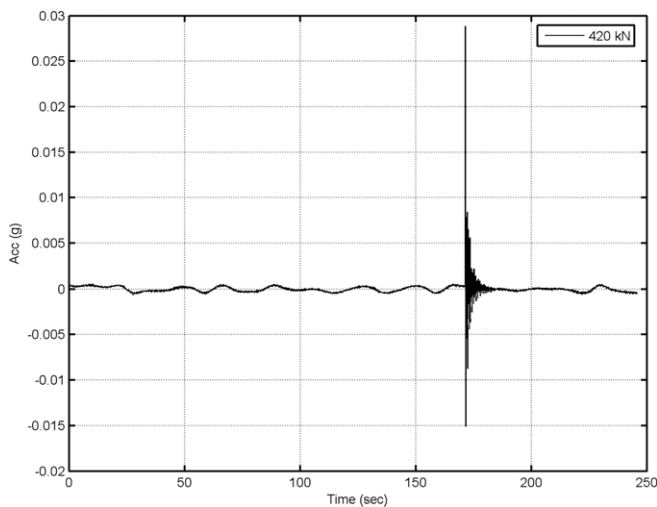Fig. 17. Stability diagram. Transverse and longitudinal sensors.

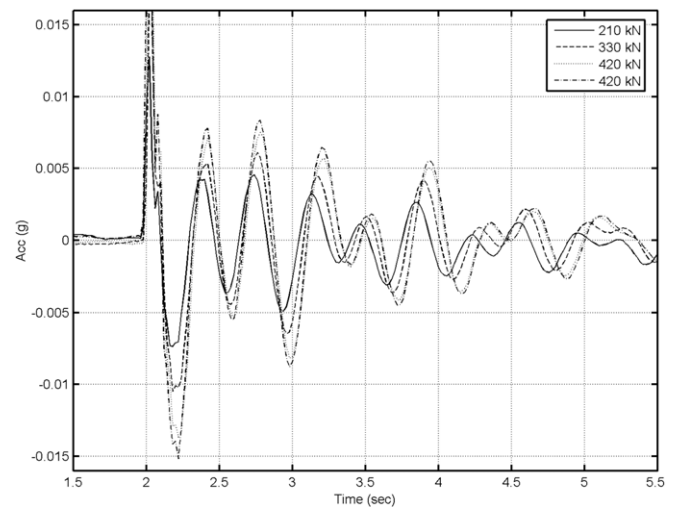Fig. 18. Ocean wave and impact induced acceleration record for 420 kN applied load.

Fig. 20. Time zoom of acceleration response to Pull-Back Test for 420 kN load.
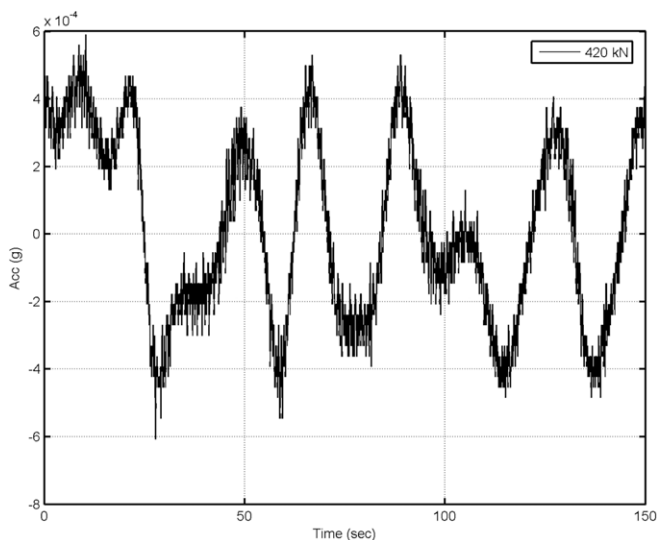
the records were filtered with a high pass filter and a low pass filter with a corner frequency of 2 Hz (Fig. 23). In this figure, it is important to note that the "low" frequency component signal has maximum amplitude of 40% of the amplitude of the "high" frequency component signal and has a latter and slower amplitude growth and decay.

Using these methods, it was determined that a period of 0.61 s (1.63 Hz) is associated with movement in the longitudinal direction. In this movement the sections involved oscillate approximately in the same direction (the phase between them is close to zero degrees). The damping for this vibration mode is in a band of 2.3%–3.1%, with a mean of 2.7% (Table 3). The decay observed in the logarithmic decrement plot is a straight line indicating that the energy dissipation for this mode can be associated with a viscoelastic system (Fig. 24). The frequency and damping variation band is small and does not show a trend with respect to the load magnitude and therefore it seems convenient to establish a single value for the entire system.

In addition, it was determined from the Pull-Back Test that there is another predominant longitudinal movement with a period that varies between 0.36 and 0.38 s (2.6–2.9 Hz). In this movement the sections involved oscillate in opposite directions (the phase between them is 180°). The damping for this vibration mode is
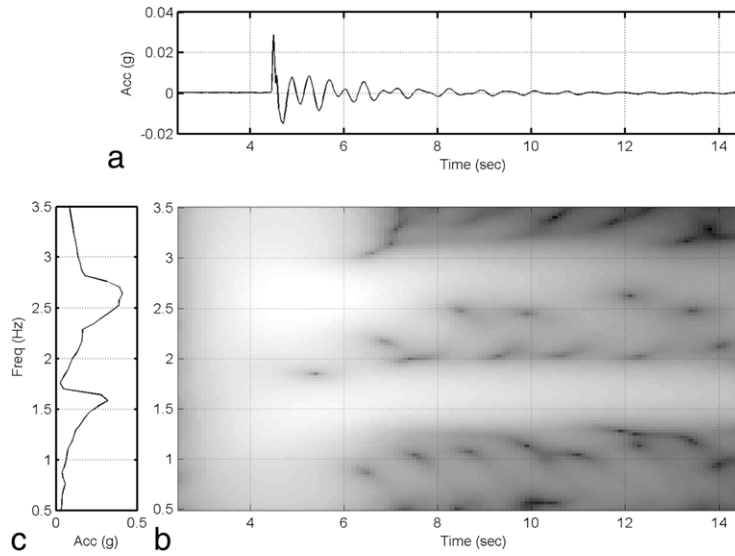

Fig. 19. Time zoom for wave induced acceleration record, for 420 kN test.

Fig. 21. Pull-Back response record and spectrogram for 420 kN. (A) Time response record. (B) Time–frequency decomposition (spectrogram). (C) Frequency response.
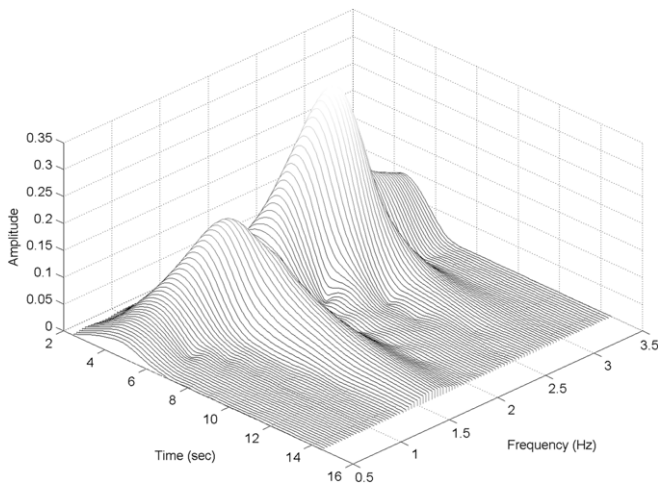

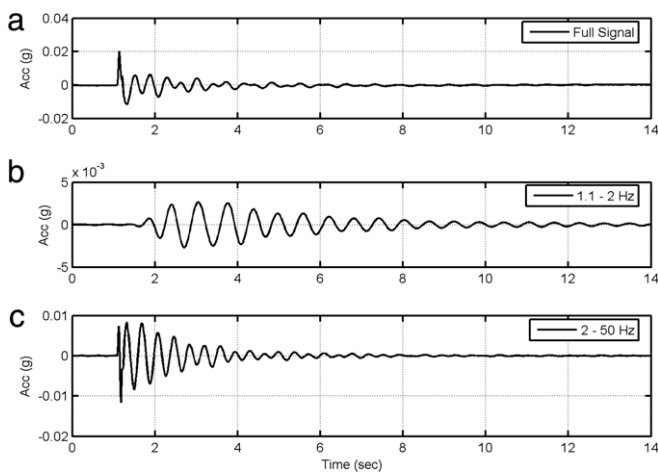**Fig. 22.** Three-dimensional view of spectrogram for the acceleration response decay after the quick release of 420 kN load.

Fig. 23. Complete and band filter signal for logarithmic decrement technique. (A) Complete signal. (B) Low pass signal. (C) High pass signal.
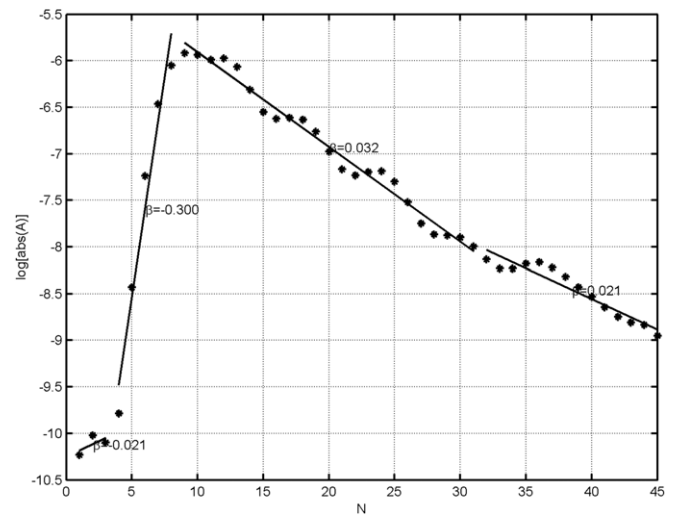
located in a band of 4.3%–4.5% with a mean of 4.4% (Fig. 25). The variation band is small and it does not show a trend with respect to

Fig. 24. Damping estimate using the logarithmic decrement technique on low frequency signal.

Table 3
Predominant frequency and observed critical damping ratio.

Applied load (kN)	ODS 1[a] Freq. (Hz)	ODS 1[a] Damping	ODS 2[a] Freq. (Hz)	ODS 2[a] Damping
100	1.633	_[b]	2.857	_[b]
100	1.664	0.028	2.796	0.043
210	1.613	0.023	2.765	0.043
330	1.633	0.026	2.722	0.043
320	1.635	0.031	2.754	0.045
420	1.602	0.026	2.686	0.043
420	1.598	0.029	2.634	0.044

[a] ODS — Operational Deflection Shape.
[b] Not identified in a reliable manner.

the load magnitude. Under this same frequency, there is a change of state in dissipation that corresponds to lower amplitudes with an equivalent critical damping ratio of 2.0%–2.5%.

The maximum displacement recorded from the Pull-Back test is nearly 2.5 mm. This value is much lower than the value expected from an analytic model of the wharf considering independent sections. This higher stiffness of the system suggests that the adjacent sections of the wharf are not independent and, at least between the sections under study, move longitudinally with a
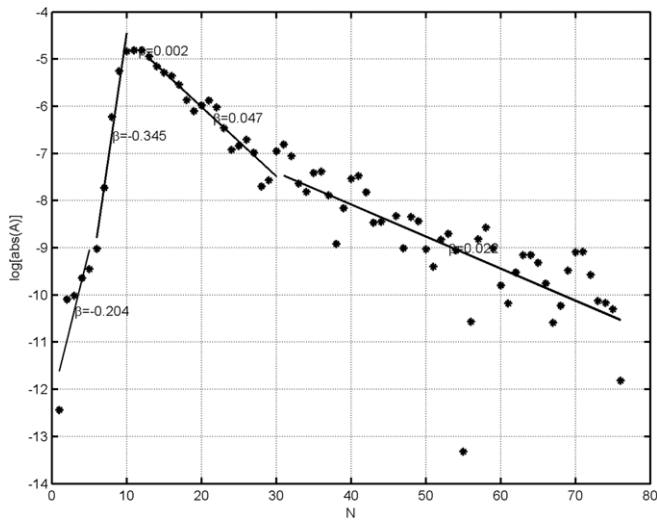
Fig. 25. Damping estimate using the logarithmic decrement technique on high frequency signal.
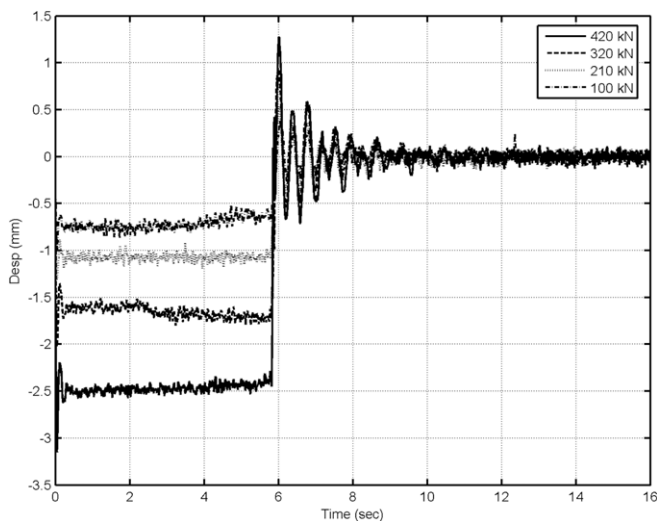

Fig. 26. Relative joint displacements between two segments at loading area. Records have been normalized to zero mean displacement at the end of the records.

certain level of coordination. This could be due to the presence of the existing frames and piping mounted on the deck or possible longitudinal friction forces due to the presence of a longitudinal steel element that is used to control transverse displacements between wharf segments. In general terms, the presence of these elements generates an integrated structural system where the individual analysis by sections in wharves, between expansion joints, is not valid. In Table 4 and Fig. 26 the relative displacements of the deck sections are shown normalized so that the mean end displacement amplitude is zero in order to perform a comparison of the response to the different applied loads. It is interesting to note from this figure that the free response has a very similar shape with different amplitudes and nearly identical oscillation periods confirming the linear behaviour previously noted.

5. Conclusions

Multiple techniques have been used to identify structural properties of the wharf studied. The methods used present different degrees of difficulty and precision.

The methods based on ambient vibrations – both parametric and non-parametric – were easy to set up and implement at

Table 4
Relative displacements between adjacent deck Sections 3 and 4 at rupture point.

Applied load (kN)	Mean displacement (mm)
100	0.6
210	1.1
320	1.7
420	2.5

the site. In general, the planning for the study required basic information about the structures to be measured and we were able to adjust the measurement procedures based on the preliminary field results.

The non-parametric frequency domain identification method using ambient vibrations required several minutes of measurements to identify the predominant frequencies and required more than 30 min before it was possible to obtain adequate results for damping. Due to the longer recording times, it was not practical to measure many points to correctly detect the modal forms and to understand the system's complexity.

The SSI parametric method shows comparable results to those of NPF and in many cases they were better than the NPF method using records that were considerably shorter in duration; generally, measurement times of 10 min per location were sufficient. An important advantage was that this method allowed us to identify operational or modal values even in cases where there was an interference of adjacent frequencies. In a particular case of this study, this method allowed the identification of frequencies and damping for a higher number of operational conditions.

The Pull-Back tests required a higher level of preparation. The study included, among other things, the evaluation of the structural drawings, machinery and piping. Predictive analytical models were developed to establish the best places to locate the pulling points, force levels, maximum acceptable displacements and type of anchoring and design of the pulling system, in order to prevent any damage. In this case, the development of this information alone took about six months. In addition, since the wharf was in operation, we had to provide a guarantee that the test would not damage the structure. Another significant inconvenience was that, due to safety reasons, the tests could only be carried out when the wharf's operations were shut down. This involved significant economic losses for the owner, ultimately limiting the time available to carry out the study.

In this case in particular, the increased level of motion imposed on the wharf did not generate important nonlinearities or modifications of predominant frequencies or damping values. Because of this the Pull-Back study at the level of force used did not contribute to the substantial improvement of the information about the system's modal properties given by ambient vibrations.

In conclusion, the ambient vibration testing was easy to perform and provided sufficient reliability and accuracy for the results presented here; the Pull-Back test was more complex to implement and did not significantly improve the quality of the data. From the data observed, we concluded the following:

1. The measured properties of the wharf were heavily influenced by the piping system, conveyor belts and other non-structural elements mounted to the deck. These "non-structural" components are generally considered as rigid structures with mass in typical design oriented analytical models. Nevertheless, our study showed that they contributed substantial stiffness and the actual behaviour of the wharf was quite different than that of the computer model generated assuming the deck sections were independent. This suggests that designers of wharf structures, at least for operational conditions, need to be careful to either provide sliding connections for the supported non-structural elements to isolate them from the wharf or else include these elements as part of their original design.

2. In general, critical damping ratios for the observed vibration levels were about 3% and 4%. This suggests that these values of damping should be used for the analysis of similar wharf structures under operating loads or low level seismic excitation.

Acknowledgements

References

[1] Benzoni G, Priestley JN. Seismic response of linked marginal wharf segments. J Earthq Eng 2003;7(4):513–39.

[2] California state land commission. Marine oil terminal engineering and maintenance standards, MOTEMS. California codes of regulations; 2005.

[3] Donahue M, Dickenson S, Miller T, Yim SC. Implications of the observed seismic performance of a pile-supported wharf for numerical modeling. Earthq Spectra 2005;21(3):617–34.

[4] Roeder C, Graff R, Soderstrom J, Han Yoo Jung. Seismic performance of pile–wharf connections. J Struct Eng 2005;131(3):428–37.

[5] Birdy J, Dodd L. Design of wharves for seismic regions. Concrete Internat 1999; 21(12):28–32.

[6] International navigation association. Seismic design guidelines for port structures. London (UK): Taylor and Francis Group; 2001.

[7] Moroni M, Sarrazin M, Boroschek R. Experiments on a base-isolated building in Santiago Chile. Eng Struct 1998;20(8):720–5.

[8] Muria-Vila D, Gomez R, King C. J Struct Eng — ASCE 1991;117(11):3396–416.

[9] Ibrahim SR, Miculcik EC. The experimental determination of vibration parameters from time response. Shock Vib 1976;46.

[10] Vega C. Damping determination of a transparent steel pier. Concrete Deck Warf. Civil engineering thesis. Santiago (Chile): Universidad de Chile; 2003 [in Spanish].

[11] Peeters B, Ventura CE. Comparative study of modal analysis techniques for bridge dynamic characteristics. Mech Syst Signal Process 2003;17(5):965–88.

[12] Diehl J. Ambient vibration survey: application. In: Theory and analytical techniques. Application Note N 3, Kinemetrics. CA (USA): Pasadena; 1993.

[13] Bendat J, Piersol AG. Engineering applications of correlation and spectral analysis. 2nd ed. New York: Wiley-Interscience; 1993.

[14] Tanaka T, Yoshizawa S, Osawa Y, Morishita T. Period and damping of vibration in actual building modes. Bull Earthq Res Inst 1969;47:1073–92.

[15] Peeters B. System identification and damage detection in civil engineering. Katholieke Universiteit Leuven — Faculteit Toegepaste Wetenschappen Arenbergkasteel, B-3001 Herlee, Belgium; 2000.

[16] Ljung L. System identification theory for the user. 2nd ed. Prentice Hall; 1999.

[17] Heylen W, Lammens SY, Sas P. Modal analysis theory and testing. Katholieke Universiteit Leuven; 1997.

[18] Allemang R, Brown D. A correlation coefficient for modal vector analysis. In: Proceedings of the 1 international modal analysis conference; 1982. p. 110–6.

[19] Van Overschee Py, De Moor B. Subspace identification for linear systems: theory – implementation – applications. Dordrecht: Kluwer Academia Publishers; 1996.